ELSEVIER

Journal of Organometallic Chemistry 655 (2002) 31–38

Journal of Organometallic Chemistry

www.elsevier.com/locate/jorganchem

Ruthenium complexes with 2,2′-, 2,4′- and 4,4′-bipyridine ligands: The role of bipyridine coordination modes and halide ligands

Toni-J.J. Kinnunen, Matti Haukka *, Eeva Pesonen, Tapani A. Pakkanen

Department of Chemistry, University of Joensuu, P.O. Box 111, FIN-80101 Joensuu, Finland

Received 15 February 2002; received in revised form 20 March 2002; accepted 22 March 2002

Abstract

Ruthenium complexes with 2,4′-bipyridine and 4,4′-bipyridine ligands, [(2,4′-bpy)$RuCl_2(CO)_3$] and [(4,4′-bpy)($RuCl_2(CO)_3)_2$], were synthesised and structurally characterised. These new complexes were compared to the well-known ruthenium compound [(2,2′-bpy)$RuCl_2(CO)_2$] by computational and experimental methods to investigate the effects of the chelating and non-chelating coordination modes of the bipyridine ligand. The stabilisation effect of the chelating 2,2′-bipyridine structure was observed. In addition to bipyridine coordination studies, theoretical studies on the effect on energy levels of changes of halide ligands in the coordination environment for ruthenium complexes were carried out showing that halides possess a significant role in the HOMO–LUMO energy gap. The ligand substitution changed especially the HOMO levels while leaving LUMOs almost intact. The computational approach was found to be a valuable aid in the design and tuning the electronic properties of ruthenium bipyridines.

Keywords: Ruthenium complexes; Bipyridine; Halide ligand

1. Introduction

Bipyridine consists of two planar pyridyl rings connected with covalent C–C bond. The schematic presentation of different bipyridines is shown in Fig. 1. The best-known isomer, 2,2′-bipyridine, typically coordinates to metal with both nitrogens yielding the chelate structure. Symmetric 4,4′-bipyridine favours a bridging bonding mode between metal centres. Transition metal compounds with 2,3′-bipyridines [1] 3,3′-bipyridines [2] and 2,4′-bipyridines [3] are less common. Non-symmetrical 2,4′-bipyridine usually coordinates as a monodentate ligand only via either N(2) or N(4′) atom, but it is also able to form bidentate bridging systems, being coordinated to two separate metal centres [4]. To our knowledge, structurally characterised ruthenium complexes with 2,4′-bipyridine have not been reported, even though it has been used together with ruthenium precursor in in situ WGSR catalysis [5].

Ruthenium complexes with 2,2′-bipyridine ligands have been thoroughly studied especially during the last decades. One of the main reasons for such wide interest is their usage as dyes in sensitised photovoltaic cells [6,7]. The photochemical properties of the dyes depend on the electronic characters of the complexes affected by the ligand systems. A simple ligand modification by varying the bipyridine substituents changes photo-electro chemical nature of the ruthenium bipyridine [8]. An even stronger effect on photo-electro chemical properties of the compound caused by the character of the halogen ligand coordinated directly to the metal centre has been observed. For example, differences in luminescence and absorption as well as redox potential (Ru^{2+}/Ru^{3+}) depending on the halogen ligand X in [Ru(4,4′-dicarboxylic acid-2,2′-bpy)$(CO)_2X_2$] have been reported [9].

In the present paper we have synthesised new ruthenium complexes with 2,4′- and 4,4′-bipyridines and studied their reactivity and stability. Theoretical and experimental methods have been applied to study

* Corresponding author. Tel.: +358-13-2513346; fax: +358-13-2513390.

E-mail address: matti.haukka@joensuu.fi (M. Haukka).

0022-328X/02/$ - see front matter
PII: S0022-328X(02)01408-0

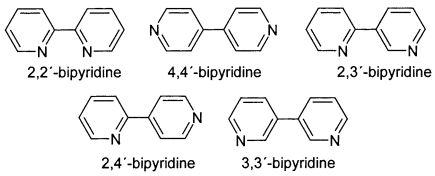

Fig. 1. Common bipyridine structures.

the differences between mono and bidentate coordination of the bipyridine ligand. The role of coordination mode on the Ru–N bond strength will be discussed. Furthermore, computational studies on compounds with different halide ligands have been used to study the dependence of highest occupied molecule orbital HOMO–LUMO energy gap on halide coordinated to the metal centre.

2. Experimental

2.1. Materials

Bipyridine complexes of Ru were synthesised from the commercial bipyridyl ligands 2,4′-bipyridine (Aldrich), 4,4′- bipyridine (Aldrich) and $[Ru(CO)_3Cl_2]_2$ (Alfa). Ligand exchange reactions were carried out by using KI (Riedel de-Haën) and KBr (Riedel de-Haën) as halogen sources.

2.2. General procedures

Syntheses were carried out air-sensitively under nitrogen and by using deoxygenated solvents. Solid reagents were used without further purification. The FT-IR spectra were measured with a Nicolet Magna-IR 750 spectrometer and the NMR spectra with a Bruker Digital NMR Avance 250 MHz. Elemental analyses were done with an EA1110 CHNS-O equipment (CE Instruments).

2.3. Synthesis of cis-(Cl)-fac(CO)-(4,4′-bipyridine)(Ru(CO)$_3$Cl$_2$)$_2$ (1)

Pre-dissolved $[Ru(CO)_3Cl_2]_2$ (3.750 g, 7.324 mmol, in 30 ml EtOH) was added to an EtOH solution of the 4,4′-bipyridine (1.144 g, 7.324 mmol, in 20 ml). The mixture was stirred for 15 min at room temperature (r.t.) and the white precipitate was filtered and washed with EtOH and then dried under vacuum. Yield: 3.660 g (75%). Anal. Found: C, 28.64; H, 1.35; N, 4.24. Calc. for $C_{16}H_8Cl_4N_2O_6Ru_2$: C, 28.76; H, 1.21; N, 4.19%. IR (in CH_2Cl_2, cm^{-1}): 2136, 2077 and 2054 (CO). δ (250 MHz, $CDCl_3$) for bpy-ring 9.20 (d, $J = 6.5$ Hz, 4H), 7.78 (d, $J = 6.8$ Hz, 4H).

2.4. Synthesis of cis-(Cl)-fac(CO)-(2,4′-bipyridine)Ru(CO)$_3$Cl$_2$ (2)

The preparation of complex **2** was carried out in a similar way as in the case of **1**. The yield of the white product was 1.379 g (65%). Anal. Found: C, 36.26; H, 2.32; N, 6.56. Calc. for $C_{13}H_8Cl_2N_2O_3Ru\cdot H_2O$: C, 36.29; H, 2.34; N, 6.51%. IR (in CH_2Cl_2, cm^{-1}): 2135, 2074 and 2051 (CO). δ (250 MHz, $CDCl_3$) for bpy-ring 9.27 (d, $J = 6.5$ Hz, 2H), 8.80 (d, $J = 4.8$ Hz, 1H), 8.17 (d, $J = 6.8$ Hz, 2H), 7.90 (d, $J = 2.8$ Hz, 2H) 7.45 (d, $J = 3.2$ Hz, 1H).

2.5. Ligand exchange experiments

Ligand exchange reactions for complexes **1** and **2** were carried out in a 100 ml Berghof autoclave equipped with a Teflon liner. Ruthenium bipyridine complex with chloride ligands (60 mg) and excess of KI or KBr were weighed and a small amount of alcohol (2 ml) solvent was added. Alternatively, the experiments were carried out with 1 ml of concentrated acids HI or HBr instead of halide salts. The closed autoclave was rapidly heated and the reaction mixture was kept at an elevated temperature of 80–200 °C for 5 h. The system was slowly (5 °C h^{-1}) cooled to ambient temperature. A corresponding method has been previously used for ligand exchange reactions for 2,2′-bipyridine complexes of ruthenium [10,11].

2.6. Formation of cis-(CO)-trans(I)-bis(2,4′-bipyridine)Ru(CO)$_2$I$_2$ (3)

Using the halogen exchange method described above, compound **2** (59.8 mg, 0.145 mmol) and the excess of KI (73.5 mg, 0.440 mmol) were heated (100 °C) in EtOH (2 ml) for 5 h yielding orange crystalline product of **3**. Yield was only some crystals. Anal. Found: C, 36.59; H, 2.41; N, 7.56. Calc. for $C_{22}H_{16}I_2N_4O_2Ru$: C, 36.53; H, 2.23; N, 7.75%. IR (in CH_2Cl_2, cm^{-1}): 2059 and 2000 (CO). δ (250 MHz, d_6-C_3H_6O) for bpy-ring.

2.7. X-ray crystallography

The X-ray diffraction data were collected on a Nonius KappaCCD diffractometer using Mo–K_α radiation ($\lambda = 0.71073$ Å) and a COLLECT [12] data collection program (**1** and **3**) or on a Nonius Mach3 diffractometer using a ω-scan data collection mode [13] and graphite monochromatised Mo–K_α radiation (**2**). For **2** the accurate cell parameters were obtained from 25 automatically centred reflections and the intensities were corrected for background and Lp factors. The DENZO and SCALEPACK [14] programs were used for cell refinements and data reduction for **1** and **3** and CAD4 EXPRESS [13]/XCAD4 [15] programs for 2. The structure **1**

was solved by the Patterson method and **2** and **3** by direct methods using the SHELXS-97 [16] or SIR-97 [17] programs with the WINGX [18] graphical user interface. Structural refinements were carried out with the SHELXL-97 [19]. All aromatic hydrogens were placed in an idealized position and constrained to ride on their parent atom. The water hydrogens in **2** were located from the difference Fourier map and refined with constant $U_{iso} = 0.05$. Compound **1** lies about an inversion centre (at the centre of the central C–C bonding the bipyridine molecule). Compound **2** has one molecule in the asymmetric unit; in compound **3** there are two independent molecules with the Ru atom in each case lying on a twofold axis. The asymmetric unit in **1** consists of half a molecule and in **2** two slightly different halves. The crystallographic data for complexes **1**–**3** are summarised in Table 2. Selected bond lengths and angles together with the values for the optimised structures are shown in Table 1. The molecular structures of complexes **1**–**3** are shown in Figs. 2–4.

2.8. Computational details

The geometries of the complexes were optimised using the B3PW91 hybrid density functional method and employing 6-31G* as a basis set (for ruthenium: Huzinaga's extra basis 433321/4331/421) [20], and the geometry optimisations were followed by analytical frequency calculations to obtain the vibration spectra and stationary point of all complexes. The calculations were carried out with GAUSSIAN-98 program [21].

Table 1
Selected bond lengths (Å) and angles (°) of complexes **1**–**3**

	Complex **1**		Complex **2**		Complex **3**	
	Experimental	Theoretical	Experimental	Theoretical	Experimental [a]	Theoretical
Bond lengths [b]						
Ru1–N1	2.160(2)	2.190	2.145(2)	2.180	2.179(4) 2.159(4)	2.219
Ru1–N2					2.179(4) 2.159(4)	2.219
Ru1–C1	1.918(3)	1.910	1.906(3)	1.900	1865(6) 1.876(6)	1.870
Ru1–C2	1.906(3)	1.910	1.913(3)	1.910	1865(6) 1.876(6)	1.870
Ru1–C3	1.914(3)	1.910	1.918(3)	1.920		
Ru1–X1	2.399(9)	2.426	2.402(1)	2.428	2.721(2) 2.703 (2)	2.740
Ru1–X2	2.391(1)	2.426	2.414(4)	2.428	2.721(2) 2.703(2)	2.750
C1–O1	1.120(4)	1.139	1.125(4)	1.139	1.142(6) 1.133(6)	1.140
C2–O2	1.121(4)	1.140	1.121(4)	1.140	1.142(6) 1.133(6)	1.140
C3–O3	1.125(4)	1.140	1.132(4)	1.140		
Bond angles [b]						
N1–Ru1–N2					87.60(2) 88.98(2)	87.02
C1–Ru1–C2	92.66(2)	95.34	92.77(1)	97.17	89.30(3) 89.00(3)	90.72
C1–Ru1–C3	91.74(1)	93.80	93.01(2)	94.09		
C2–Ru1–C3	93.13(1)	93.60	91.14(2)	94.05		
X1–Ru1–X2	89.04(3)	92.53	91.03(3)	91.37	177.03(3) 177.14(3)	176.67
Ru1–C1–O1	177.70(3)	177.53	178.90(3)	177.61	179.70(5) 179.50(6)	179.08
Ru1–C2–O2	174.10(3)	178.91	178.80(3)	178.84	179.70(5) 179.50(6)	179.06
Ru1–C3–O3	175.30(3)	178.88	177.30(3)	178.85		

[a] The asymmetric unit contains two molecules.
[b] In complex **3**, the labels (1A) in Fig. 3 corresponds to the label number 2 used in this table.

Table 2
Crystallographic data for complexes **1**–**3**

Compound	**1**	**2**	**3**
Empirical formula	$C_{16}H_8Cl_4N_2O_6Ru_2$	$C_{13}H_{10}Cl_2N_2O_4Ru$	$C_{22}H_{16}I_2N_4O_2Ru$
Formula weight	668.18	430.20	723.26
Temperature (K)	293(2)	293(2)	150(2)
Wavelength (Å)	0.71073	0.71073	0.71073
Crystal system	Monoclinic	Orthorhombic	Orthorhombic
Space group	$P21/c$	$P2_12_12_1$	$Pccn$
a (Å)	5.9660(2)	7.3362(4)	21.9608(5)
b (Å)	12.6390(6)	12.3274(7)	10.6181(2)
c (Å)	14.5843(5)	17.7039(15)	20.1734(4)
α (°)	90	90	90
β (°)	97.498(3)	90	90
γ (°)	90	90	90
V (Å^3)	1090.32(7)	1601.1(2)	4704.1(2)
Z	2	4	8
D_{calc} (g cm^{-3})	2.035	1.785	2.042
Absorption coefficient (mm^{-1})	1.910	1.329	3.317
$F(000)$	644	848	2736
Crystal size (mm)	0.2 × 0.1 × 0.1	0.3 × 0.3 × 0.3	0.2 × 0.2 × 0.2
Theta range for data collection (°)	3.44–28.21	2.01–24.99	3.70–25.50
Index ranges	$-7 \le h \le 7$, $-16 \le k \le 16$, $-19 \le l \le 19$	$-1 \le h \le 8$, $-1 \le k \le 14$, $-1 \le l \le 21$	$-26 \le h \le 26$, $-12 \le k \le 12$, $-24 \le l \le 24$
Reflections collected	4944	2211	8238
Independent reflections	2537	2039	4367
R_{int}	0.0194	0.0084	0.0224
R_1 [$I > 2\sigma(I)$]	0.0301	0.0167	0.0322
wR_2 [$I > 2\sigma(I)$]	0.0691	0.0445	0.0721
wR_2 (all data)	0.0744	0.0451	0.0810
Goodness-of-fit on F^2	1.041	1.092	1.123
Largest difference peak and hole (e Å^{-3})	0.674 and −0.835	0.209 and −0.416	0.885 and −0.908

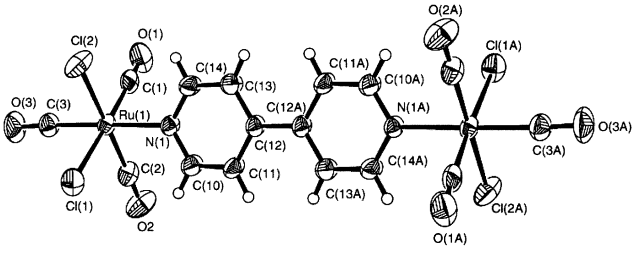

Fig. 2. Molecular structure of complexes **1**. The thermal ellipsoids are drawn at the 50% probability level.

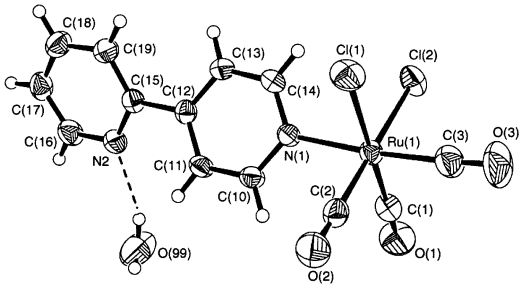

Fig. 3. Molecular structure of complex **2**. The thermal ellipsoids are drawn at the 50% probability level.

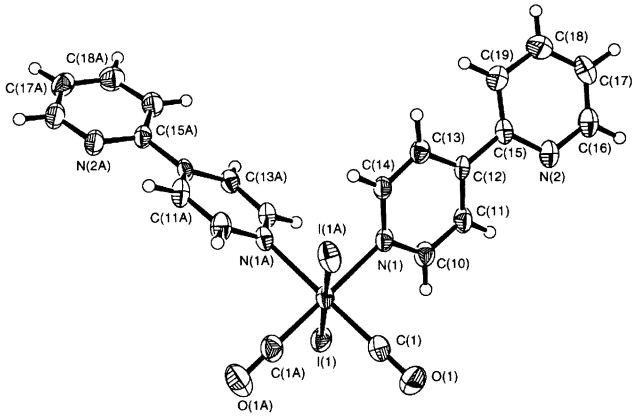

Fig. 4. Molecular structure of one of the molecules of complex **3**. The thermal ellipsoids are drawn at the 50% probability level.

3. Results and discussion

3.1. Chelating effects

Simple ligand replacement reactions in an autoclave have been previously used to produce a series of 2,2′-bipyridine complexes of ruthenium [10,11]. In those experiments the main structure of [(2,2′-bipyridine)

$RuCl_2(CO_2)$] was not severely decomposed even at 240 °C in acidic conditions. However, all our experiments with [(2,4′-bipyridine)$RuCl_2(CO)_3$] and [(4,4′-bipyridine)($RuCl_2(CO)_3)_2$] led to cleavage of Ru–N bond, and at least partial degradation of the original bipyridine complexes. The decomposition had already occurred in both acidic and neutral conditions at the relatively low temperature of 80 °C for both **1** and **2** and both iodide and bromide experiments. The most probable reason for the decomposition in the case of 2,4′- and 4,4′-bipyridine complexes is the absence of the stabilising N–N chelate structure. The crystal structure of **3** shows that halogen exchanges have occurred indeed, but either before or after the metal detaches from the bipyridine ligand.

The experimentally observed differences between monodentate and chelating N–Ru interactions were studied by computational methods to clarify the character of the interactions between nitrogen and ruthenium. Clear differences have also been obtained in computational studies on bond strengths. The lengths of the Ru–N bonds in the bipyridine complexes summarised in Table 3 indicates that the chelating structure increases the Ru–N interaction; bond lengths in complexes with monodentate ligand bonding are systematically longer (2.18–2.20 Å) than in 2,2′-bipyridine complexes (2.15 Å). The shortness of the Ru–N bond length for the chelating 2,2′-bipyridine species most probably relates to the increased π-back bonding compared to monodentate coordination modes.

The lowest energy absorption band in the UV–vis spectrum for ruthenium bipyridine compounds refers typically to metal to ligand charge transfer (MLCT) and the bipy coordination mode was observed to have an influence on the energy of this electron transfer. The lowest energy band for bidentate coordinated 2,2′-bipyridine species is on the boundary line of UV–vis regions, while for both complexes **1** and **2** without chelating coordination, the required energy for MLCT is higher yielding lower λ_{max} values. The absorption spectrum data are summarised in Table 4.

3.2. Halide exchanges

The well-known dependence [9,22] between the photo-electrochemical properties of the ruthenium bipyridines and the characters of the ligands coordinated to the metal was observed also in our studies. Halogen substitution in ruthenium mono (bipyridine) has an effect on the electronic properties of the compound. In ruthenium bipyridine systems, the HOMO contains ruthenium d-orbitals and the lowest unoccupied (LUMO) is typically π*-orbital of the bipyridine ring. The energy gap between HOMO and LUMO depends on halogen coordinated to Ru; calculated energies are shown in Table 3. For all studied systems, the replacement of chlorides with other halide ligands, bromides or iodides, reduced the gap raising the value of ruthenium d-orbital, as seen in Fig. 5. In the case of [(2,4′-bipyridine)($RuX_2(CO)_3)_2$] and [(2,4′-bipyridine)($RuX_2(CO)_3)_2$] (X = Cl, Br, I) the HOMO–LUMO energy gap is decreasing in order Cl > Br > I. However, in the [(2,2′-bipyridine)$RuX_2(CO)_2$] the order is Cl > I > Br. This deviant behaviour of iodine substituted 2,2′-bipyridine species is due to different effect of the halide exchange in metal coordination sphere, as seen in Table 3. The exceptional photo-electrochemical behaviour of

Table 3
Absorption maxima for methanol and acetonitrile solutions of ruthenium complexes with different bipyridine ligands

Complex	λ_{max} (nm)	
	Methanol	Acetonitrile
[(2,2′-bpy)$RuCl_2(CO)_2$]	342	351
[(2,4′-bpy)$RuCl_2(CO)_3$]	281	282
[(4,4′-bpy)($RuCl_2(CO_3)_2$]	262	266

Table 4
HOMO–LUMO energy differences and Ru–N bond lengths of optimised ruthenium bipyridine complexes with halogen X ligands [a]

Complex	ΔE (HOMO–LUMO) (eV)	Ru–N (Å)
[(2,2′-bpy)$RuCl_2(CO)_2$]	3.13	2.156
[(2,2′-bpy)$RuBr_2(CO)_2$]	2.88	2.155
[(2,2′-bpy)$RuI_2(CO)_2$]	2.89	2.156
[(2,4′-bpy)$RuCl_2(CO)_3$]	4.21	2.180
[(2,4′-bpy)$RuBr_2(CO)_3$]	3.83	2.190
[(2,4′-bpy)$RuI_2(CO)_3$]	3.47	2.205
[(4,4′-bpy)($RuCl_2C(CO)_3)_2$]	3.82	2.190
[(4,4′-bpy)($RuBr_2(CO)_3)_2$]	3.51	2.205
[(4,4′-bpy)($RuI_2(CO)_3)_2$]	3.05	2.224

[a] Calculated with B3PW91 method.

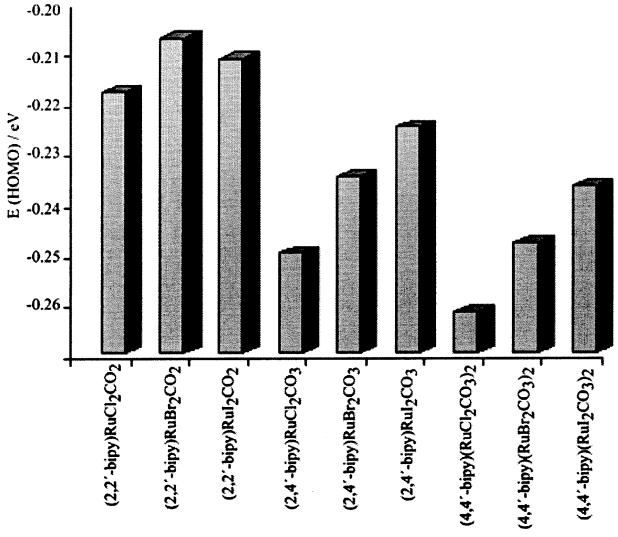

Fig. 5. The energies of HOMO of ruthenium bipyridines affected by halide ligands.

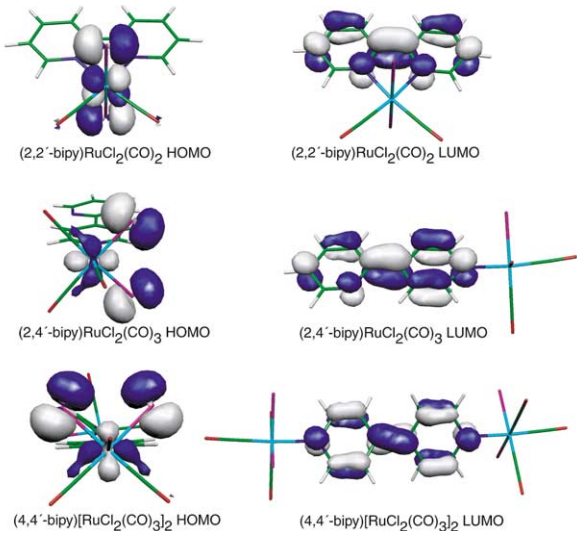

Fig. 6. Graphic presentation of HOMO and LUMO orbitals of Ru bipyridines.

iodide substituted compound has been reported earlier [9].

The strong influence of halide ligand on the electron density distribution of the complexes can easily be seen by considering the structure of HOMO of ruthenium(II) bipyridines. The highest occupied orbital consists of a mixture of Ru d-orbitals and halogen p-orbitals. The combination of these two atom orbitals has an anti-bonding character as it can be seen from the graphic presentation of the HOMO orbitals (Fig. 6). Each halide substituent has the specific nature of its p-orbital and therefore the whole HOMO is affected by halogen variation. Correspondingly, the LUMO is located in the bipyridine system and therefore it is more or less independent of the halide substituents. Hence, the dependence of the energy gap between the occupied and unoccupied orbital on the halide substituent is mainly due to variation of HOMO levels.

3.3. Crystal packing

Compared to the computationally optimised isolated molecules, the experimental crystal structures of the 2,4′- and 4,4′-bipyridine complexes of ruthenium showed some geometrical differences due to intermolecular interactions. In the crystal structure of **2** the pyridine rings of the bipyridine ligand are twisted off plane. The angle between the ring planes is 25.87(7)°. Both pyridine units form almost parallel stacks with the neighbouring molecule (Fig. 7). The angle between the neighbouring ring planes (N(1)···C(10)···C(14) and N(2#)···C(15#)···C(19#) in equivalent position # = −0.5+*X*,1.5−*Y*, 1−*Z*) is 2.9° and the distances between the closest centroids of the pyridine rings 3.721 and 3.742 Å (N(1)···C(10)···C(14)–N(2#)···C(15#)···C(19#) and N(2)···C(15)···C(19)–N(1#)···C(10#)···C(14#), respectively; equivalent position # = −0.5+*X*, 1.5−*Y*, 1−*Z*). In respect to the bipyridine ligand arrangement, the crystal structure of **3** resembles the structure of **2**. The pyridine rings are again off plane. In **3** the angle between the ring planes in two molecules found in the asymmetric unit are 21.7(3) and 13.7(3)°, respectively. Stacking is also observed in **3**, but in this case only the two closest neighbouring rings are stacked while the next ring system is already further away (Fig. 8). The angles between the closest neighbouring ring planes are 3.4° (between the rings N(2)···C(15)···C(19) and N(1B#)···C(10B#)–C(14B#)) and 7.1° (between the rings N(1)···C(10)···C(14) and N(2B#)···C(15B#)···C(19B#), where # = 1−*X*, 2−*Y*, −*Z*) and the centroid distances 3.609 and 3.782 Å, respectively. The next closest centroid distance is already much longer 4.624 Å (between the rings N(2B#)···C(15B#)···C(19B#)–N(2#)···C(15#)···C(19#), where #2 = *X*, −1+*Y*, *Z*). A true stacking of the pyridine rings does not occur in **1**. The shortest distances between the closest ring centroids are considerably longer (5.506 and 5.966 Å for N(1)···C(10)···C(14)–N(1#)···C(10#)···C(14#) # = 1−*X*, 1−*Y*, −*Z* and N(1)···C(10)···C(14)–N(1#2)···C(10#2)···C(14#2), #2 = 1+*X*, *Y*, *Z*, respectively) than in **2** or **3**.

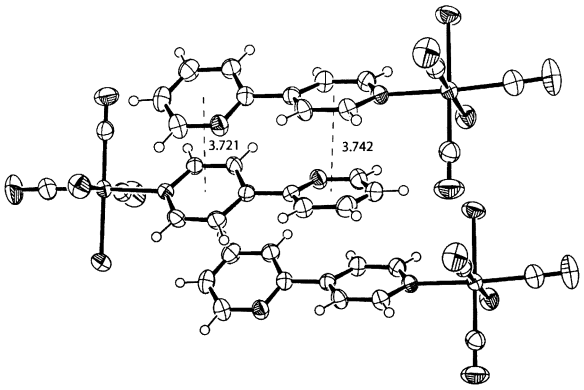

Fig. 7. Packing of [Ru(2,4′-bpy)(CO)3Cl2] (distances in Å).

In both **2** and **3** the 2,4′-bipyridine acts as a monodentate ligand. It is coordinated to the ruthenium via only one nitrogen atom. In **2** a water molecule is hydrogen bonded to the non-coordinated nitrogen with

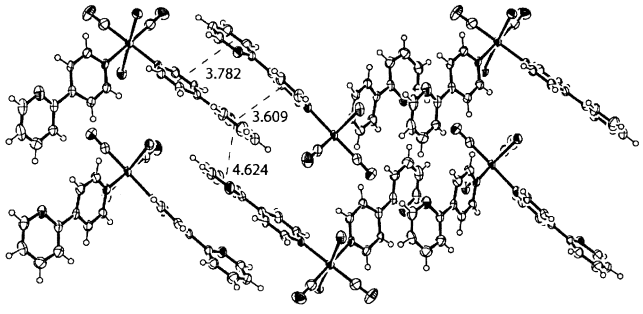

Fig. 8. Packing of [Ru(2,4′-bpy)2(CO)2I2] (distances in Å).

O···N distance of 2.892(4) Å. In **3** the neighbouring pyridine ring blocks the non-coordinated nitrogen. The closest C_{arom}···N distance is only 3.723 Å with C–H···N angle of 168.3°. Although this is not a classical hydrogen bond, the close vicinity of the neighbouring ring prevents any solvent coordination.

4. Conclusions

The nature of bipyridine coordination to ruthenium has an effect on the Ru–N bond strength. The chelating coordination of bidentate coordinated 2,2′-bipyridine stabilises ruthenium complexes compared to monodentate 2,4′-bipyridine and 4,4′-bipyridine compounds. The stronger Ru–N interactions in chelating complexes can be seen as shorter bond lengths between ruthenium and nitrogen atoms. The obtained results of the coordination mode differences could be exploited, for example in the selection of ligand for catalytic purposes.

Computational chemistry provides a fast and convenient aid for the prediction of metal complex behaviour as a function of compound manipulations. The energy gap between occupied and unoccupied orbitals is essentially connected to photo-electrochemical characteristics, such as absorption and luminescence properties. The role of halide ligands in photo-electrochemical behaviour is obvious, because the molecular orbitals participating the electron transfers, i.e. HOMO is mainly composed of metal d and halogen p-orbitals. Each halide has own electronic characteristic and therefore the halide exchange changes the energy gap between HOMO and LUMO.

5. Supplementary material

Crystallographic data for the structural analysis have been deposited with the Cambridge Crystallographic Data Centre, CCDC nos. 174747–174749 for complexes **1**–**3**, respectively. Copies of these data may be obtained free of charge from The Director, CCDC, 12 Union Road, Cambridge CB2 1EZ, UK (Fax: +44-1223-336033 or e-mail: deposit@ccdc.cam.ac.uk or www: http://www.ccdc.cam.ac.uk.

Acknowledgements

Financial support by a grant from the Academy of Finland (M.H.) is gratefully acknowledged.

References

[1] Y. Chen, S. Songsheng, E. Rex, Transition Met. Chem. (London) 22 (1997) 338.
[2] Chosen examples: (a) E.C. Constable, D. Morris, S. Carr, New J. Chem. 22 (1998) 287;
(b) R.L. LaDuca Jr., C. Brodkin, R.C. Finn, J. Zubieta, Inorg. Chem. Commun. 3 (2000) 248;
(c) S.L. McWhinnie, J.A. Thomas, T.A. Hamor, C.J. Jones, J.A. McCleverty, D. Collison, F.E. Mabbs, C.J. Harding, L.J. Yellowlees, M.G. Hutchings, Inorg. Chem. 35 (1996) 760;
(d) R.L. LaDuca Jr., M. Desciak, M. Laskoski, R.S. Rarig Jr., J. Zubieta, J. Chem. Soc. Dalton Trans. (2000) 2255;
(e) S. Lopez, M. Kahraman, M. Harmata, S.W. Keller, Inorg. Chem. 36 (1997) 6138.
[3] (a) D. Czakis-Sulikowska, J. Katuzna, J. Therm. Anal. 47 (1996) 1763;
(b) J. Radwanska-Doczekalska, D. Czakis-Sulikowska, M. Markiewicz, J. Therm. Anal. 48 (1997) 865;
(c) D. Czakis-Sulikowska, J. Radwanska-Doczekalska, M. Markiewicz, J. Therm. Anal. Cal. 60 (2000) 145;
(d) D. Czakis-Sulikowska, J. Katuzna, J. Radwanska-Doczekalska, J. Therm. Anal. 54 (1998) 103;
(e) D. Czakis-Sulikowska, J. Katuzna-Czaplinska, Pol. J. Chem. 72 (1998) 2218;
(f) D. Czakis-Sulikowska, J. Radwanska-Doczekalska, M. Markiewicz, N. Pustelnik, B. Kuznik, Pol. J. Chem. 71 (1997) 513;
(g) Z. Wang, R.-G. Xiong, E. Naggar, B.M. Foxman, W. Lin, Inorg. Chim. Acta 288 (1999) 215;
(h) W.-Y. Wong, W.-T. Wong, S.-Z. Hu, Inorg. Chim. Acta 234 (1995) 5.
[4] M.-L. Tong, X.-M. Chen, B.-H. Ye, S. Weng Ng, Inorg. Chem. 37 (1998) 5278.
[5] T. Venäläinen, T.A. Pakkanen, J. Mol. Catal. 59 (1990) 33.
[6] Pioneering work: B. O'Regan, M. Grätzel, Nature 353 (1991) 737.
[7] (a) O. Kohle, S. Ruile, M. Grätzel, Inorg. Chem. 35 (1996) 4779;
(b) M. Grätzel, Platinum Metals Rev. 38 (1994) 151;
(c) M.K. Nazeeruddin, A. Kay, I. Rodicio, R. Humphry-Baker, E. Müller, P. Liska, N. Vlachopoulos, M. Grätzel, J. Am. Chem. Soc. 115 (1993) 6382.
[8] (a) P.A. Anderson, R.F. Anderson, M. Furue, P.C. Junk, F.R. Keene, B.P. Patterson, B.D. Yeomans, Inorg. Chem. 39 (2000) 2721;
(b) N.H. Damrauer, J.K. McCusker, Inorg. Chem 38 (1999) 4268;
(c) A.E. Curtright, J.K. McCusker, J. Phys. Chem. 103 (1999) 7032;
(d) C. Caix-Cecillon, S. Chardon-Noblat, A. Deronzier, M. Haukka, T.A. Pakkanen, R. Ziesel, D. Zsoldos, J. Electroanal. Chem. 466 (1999) 187;
(e) R.-A. Fallahpour, Eur. J. Inorg. Chem. (1998) 1205;
(f) A. Basu, M.A. Weiner, T.C. Strekas, H.D. Gafney, Inorg. Chem. 21 (1982) 1085;
(g) T.-J.J. Kinnunen, M. Haukka, M. Nousiainen, A. Patrikka, Tapani A. Pakkanen, J. Chem. Soc. Dalton Trans. (2001) 2649.
[9] S. Luukkanen, M. Haukka, E. Eskelinen, T.A. Pakkanen, V. Lehtovuori, J. Kallioinen, P. Myllyperkiö, J. Korpi-Tommola, Phys. Chem. Chem. Phys. 3 (2001) 1992.
[10] P. Homanen, M. Haukka, S. Luukkanen, M. Ahlgrén, T.A. Pakkanen, Eur. J. Inorg. Chem. (1999) 101.
[11] P. Homanen, M. Haukka, T.A. Pakkanen, J. Pursiainen, R.H. Laitinen, Organometallics 15 (1996) 4081.
[12] COLLECT data collection software, Nonius B.V., 1997–2000.
[13] CAD4 Express Software, Enraf-Nonius, Delft, The Netherlands, 1994.
[14] Z. Otwinowski, W. Minor, DENZO-SCALEPACK, Processing of X-ray diffraction data collected in oscillation mode, in: C.W. Carter

Jr., R.M. Sweet (Eds.), Methods in Enzymology, vol. 276, Macromolecular Crystallography, Part A, Academic Press, New York, 1997, pp. 307–326.
[15] K. Harms, S. Wocadlo, XCAD4–CAD4 Data Reduction, University of Marburg, Marburg, Germany, 1995.
[16] G.M. Sheldrick, SHELXS-97, Program for Crystal Structure Determination, University of Göttingen, 1997.
[17] A. Altomare, M.C. Burla, M. Camalli, G.L. Cascarano, C. Giacovazzo, A. Guagliardi, A.G. Moliterni, G. Polidori, R.J. Spagna, J. Appl. Crystallogr. 32 (1999) 115.
[18] L.J. Farrugia, J. Appl. Crystallogr. 32 (1999) 837.
[19] G.M. Sheldrick, SHELXL-97, Program for Crystal Structure Refinement, University of Göttingen, Germany, 1997.
[20] S. Huzinaga (Ed.), Gaussian Basis Sets for Molecular Calculations, Physical Sciences Data 16, Elsevier, Amsterdam, 1984.
[21] M.J. Frisch, G.W. Trucks, H.B. Schlegel, G.E. Scuseria, M.A. Robb, J.R. Cheeseman, V.G. Zakrzewski, J.A. Montgomery Jr., R.E. Stratmann, J.C. Burant, S. Dapprich, J.M. Millam, A.D. Daniels, K.N. Kudin, M.C. Strain, O. Farkas, J. Tomasi, V. Barone, M. Cossi, R. Cammi, B. Mennucci, C. Pomelli, C. Adamo, S. Clifford, J. Ochterski, G.A. Petersson, P.Y. Ayala, Q. Cui, K. Morokuma, D.K. Malick, A.D. Rabuck, K. Raghavachari, J.B. Foresman, J. Cioslowski, J.V. Ortiz, A.G. Baboul, B.B. Stefanov, G. Liu, A. Liashenko, P. Piskorz, I. Komaromi, R. Gomperts, R.L. Martin, D.J. Fox, T. Keith, M.A. Al-Laham, C.Y. Peng, A. Nanayakkara, C. Gonzalez, M. Challacombe, P.M.W. Gill, B. Johnson, W. Chen, M.W. Wong, J.L. Andres, C. Gonzalez, M. Head-Gordon, E.S. Replogle, J.A. Pople, Gaussian, Inc., Pittsburgh, PA, 1998.
[22] See for example: (a) A. Juris, V. Balzani, F. Barigelletti, S. Campagna, P. Belser, A. von Zelewsky, Coord. Chem. Rev. 84 (1988) 85;
(b) P.A. Anderson, G.B. Deacon, K.H. Haarmann, F.R. Keene, T.J. Meyer, D.A. Reitsma, B.W. Skelton, G.F. Strouse, N.C. Thomas, J.A. Treadway, A.H. White, Inorg. Chem. 34 (1995) 6145;
(c) Md.K. Nazeeruddin, S.M. Zakeeruddin, R. Humphry-Baker, S.I. Gorelsky, A.B.P. Lever, M. Grätzel, Coord. Chem. Rev. 208 (2000) 213.